WARSAW UNIVERSITY OF TECHNOLOGY Index 351733
FACULTY OF CIVIL ENGINEERING
COMMITTEE FOR CIVIL AND WATER ENGINEERING
POLISH ACADEMY OF SCIENCES ISSN 1230-2945

DOI: 10.24425/ace.2023.147664

ARCHIVES OF CIVIL ENGINEERING

Vol. LXIX ISSUE 4 2023

pp. 359 –377

Research paper

Experimental investigations of steel cold-formed moment-resisting bolted lap joints under monotonic and cyclic loading

Rafał Budziński[1], Lucjan Ślęczka[2]

Abstract: Joints in cold-formed steel framing structures are usually designed as bolted lap type ones with a gusset plate. Unlike the end-plate joints in hot-rolled structures, the load in such joints is transferred through shearing of the bolts and bearing of the material. The prediction of their structural properties may be problematic in view of unfavourable influence of the hole clearance and hole ovalization resulting from low bearing resistance of thin walls. A few experimental programmes showed that these issues lead to a different behaviour of the whole joint comparing to common end plate type. These concerns may be particularly important for joints under variable loading, which are prone to deterioration of structural properties. The testing programme conducted by the authors was focused on their behaviour under monotonic and cyclic loading with attention to a potential drop of resistance and stiffness. Monotonic tests revealed quite similar course of the joints' response. In view of high deformability of the specimens at the intermediate stage of each monotonic test, plastic moment resistances of joints were associated with the initial part of the moment-rotation curves and were multiple times lower than maximum moments obtained in the experiments. The quantities of deterioration of structural properties were determined based on cyclic tests. Drop of resistance and stiffness was observed for several levels of loading range, but the trend of decrease varied for each property. Application of the DIC technique allowed one to identify qualitatively and quantitatively the sources of joint deformability.

Keywords: bolted lap connections, cold-formed steel, cyclic loading, initial stiffness, steel joints

[1]MSc, Eng., Rzeszow University of Technology, Faculty of Civil and Environmental Engineering and Architecture, Al. Powstańców Warszawy 12, 35-959 Rzeszów, Poland, e-mail: r.budzinski@prz.edu.pl, ORCID: 0000-0002-9890-845X

[2]PhD, DSc, Eng., Rzeszow University of Technology, Faculty of Civil and Environmental Engineering and Architecture, Al. Powstańców Warszawy 12, 35-959 Rzeszów, Poland, e-mail: sleczka@prz.edu.pl, ORCID: 0000-0002-8979-7073

1. Introduction

Cold-formed steel (CFS) is becoming more and more common in various framing systems, ranging from light gauge steel framing in residential construction to single storey industrial buildings of moderate span. The specificity of the design of CFS sections demands a different approach to shaping of the structure comparing to hot-rolled steel. It results from different assortment of cross-sections and the need to limit various forms of buckling on the local and global level. In this context, the most popular solution for framing members is a double channel section in the back-to-back position [1, 2]. Different types of cross-section profiles also require alternative solutions for joint shaping. The need of their proper design is particularly essential for frames, in which joints characteristics greatly affects the structural systems response towards bending moment distribution, deformations and critical loads [3].

Currently, the majority of steel joints designed, both in hot-rolled and CFS structures, are treated as semi-rigid [4,5]. Consequently, the derivation of their characteristics resulting from the moment-rotation relationship is essential to obtain the actual global response of the structure. EN 1993-1-8 standard [6] gives the possibility to calculate the resistance and stiffness of steel joints based on the component method. This algorithm is dedicated to end-plate joints in hot-rolled structures consisting of I- or H-sections.

In case of the aforementioned CFS cross-section, the joints are usually based on bolted lap-type ones with the usage of a gusset plate. These joints transfer loads through shearing of the bolts. The moment resistance of lap joints is obtained through sufficient number of bolts and distances between them. A few studies focused on the application of the component method in order to assess the structural properties for such joints revealed their complex behaviour [5, 7–9]. The failure is often caused from buckling and therefore differ from the typical forms obtained in lap connections used in hot-rolled structures [10]. The most common forms of failure for described CFS joints are as follows: local buckling of the member [8, 9, 11, 13], buckling of the gusset plate [7, 12, 13] and bearing of the bolts [5, 8, 12]. Low stiffness of thin walls of the member occurs to be one of the problems in achieving the expected capacity in moment resisting CFS joints. Another potentially weakest component, which is not directly included in the component method approach, is a gusset plate. Depending on the joint shaping, the gusset plate can reach large sizes in joints with many bolts, which makes it susceptible to lateral buckling. Klich et. al. [7] applied a stiffness formula for free edge gusset plate in compression from the Martin & Robinson study [14] in their analytical approach based on the component method. However when it comes to CFS joint responsible for resisting large bending moments, the gusset plate is stiffened with welded or folded inner flange [8]. A solution for the computational representation of the stiffness of such gusset plate has not been so far sufficiently described.

The complexity and dissimilarity in the approach to CFS joints comparing to hot-rolled ones results not only from high sensitivity to buckling, but also the characteristics of lap joints. They are made with hole clearances, which are specified in the technical requirements [15]. This induces a gap between the unloaded bolts and the member's wall. Considering CFS structures, these connections are usually designed as Category A ac-

cording to EN 1993-1-8 standard [6]. This means no pretensioning of the bolts and no requirement of torque control. Consequently, a small friction between the parts of the connection is overcome at minor loading, which induces slip and eventually the additional rotation in moment resisting joints. Moreover, large displacements within the lap connections might also result from bearing of the bolts. Due to thin walls of CFS sections, this case is mainly responsible for the resistance of each connection and the whole joint. Also for this reason, the deformability of the joint may be unfavourably impacted by the hole ovalization. Henriques et al. [16] considered these issues with the geometrical imperfections in the study of analytical and numerical model of shear lap connection. Non-fitted bolts combined with bearing failure mechanism were evaluated as damaging for plastic resistance development and ductility requirements. These effects might be especially undesired combined with variable loading, which was the subject of the numerical studies by several authors [17–20]. The authors focused on the model of friction-slip mechanism, which was found to be crucial for sufficient ductility and energy dissipation capacity of the joint. Cyclic tests on CFS joints conducted by Dubina et al. [8] confirmed, that the phenomenon of bolts slippage has a significant impact on the joints behaviour. The failure was observed due to ovalization of the holes, thus exhausting the bearing resistance. What is more, a deterioration of the joint properties was also observed with successive cycles.

The paper presents results of an experimental investigation of the flexural behaviour of eaves joints under monotonic and cyclic loading. The structural properties of the joints were determined under monotonic loads and their deterioration under variable load conditions were investigated. The novelty described in the paper is the application of DIC technique (Digital Image Correlation), which allowed one to identify qualitatively and quantitatively the sources of joint deformability.

2. Experimental investigation of CFS joints under bending

2.1. Testing stand

The testing stand was designed for static testing of steel joints under bending moment in two directions. The stand was prepared for specimens consisting of vertical and horizontal member, performing a portal frame rafter and column in a “knee” shaped structure, respectively. The connection made between these members constituted a joint that was the subject of the experimental study. The load of a certain direction was transmitted horizontally through the use of Instron-Schenck 630 kN hydraulic jack, fixed in a rigid, robust column. The load was applied at the free end of the vertical member, which generated bending moment in the analysed joint. The load from the joint was transferred to a horizontal member that was fixed to the strong floor by two simple supports. Moreover the structure was restraint with lateral supports in 4 locations outside the joint area in order to prevent global forms of buckling. Due to the need to replicate the eaves joint of the actual frame, the members were designed at an angle to simulate a roof pitch of 10 degrees. The simplified static scheme and view of the testing stand is shown in Fig. 1.

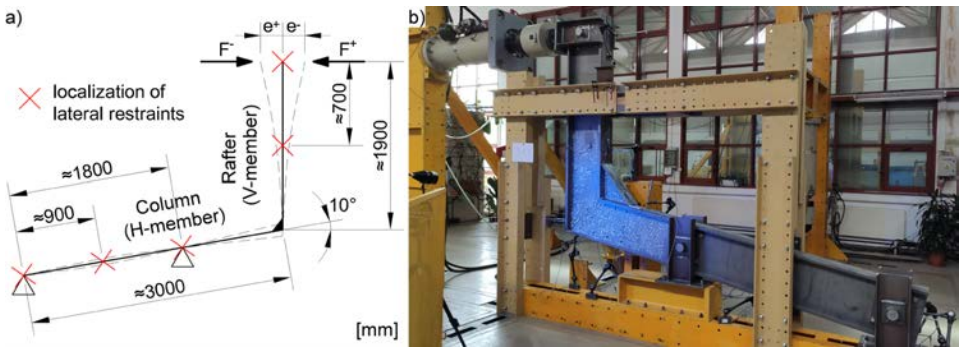

Fig. 1. The testing stand: a) simplified static scheme and b) view of the testing stand

2.2. Bolted lap joint specimens

The introduced tests specimens were joining built-up members consisting of two channel sections with the height of 450 mm and made from 4 mm sheets of S355 steel grade. The joints were designed with gusset plates of 10 mm thickness placed in the gap between the two sections. The gusset plates had and additional welded flange in the inner corner of the joint in order to strengthen this component against buckling. The joints were made by connecting the channel webs to the gusset plate on the column and rafter side with M16 bolts class 8.8 with partially threaded shank. In that way, the joint is designed to transmit bending moment by shearing of the bolts and bearing of the walls of the components to be joined in one plane coinciding with the plane of the frame. The selected shape of the joint and the dimensions of the cross section of the connected members were similar to the structural solution used by a local contractor of single storey steel industrial buildings, who was the supplier of the specimens. The joints have been executed as Category A bolted connections, assuming load transfer through bearing and no pretensioning of the bolts. However, the bolts were assembled with same controlled torque of 60 N·m, which approximately refer to 25% of the tightening moment for preloaded bolts.

Two geometries, differing in the number and spacing of the bolts, were prepared for experimental testing. The introduced S 1 and S 2 type specimens consisted of 18 and 14 bolts, respectively. The geometry of both variants is presented in Fig. 2. A total of 6 samples were tested – 3 for each option presented.

2.3. Testing instrumentation

The applied force and the displacement of the hydraulic jack piston were registered by the integrated sensors of the Instron Schenck testing system. Other instrumentation of the testing stand consisted of a set of LVDT displacement sensors, which controlled in plane and out of plane displacements of the specimen and the rigid stationary parts of the stand. Several strain gauges were used in certain locations including flanges of channel sections

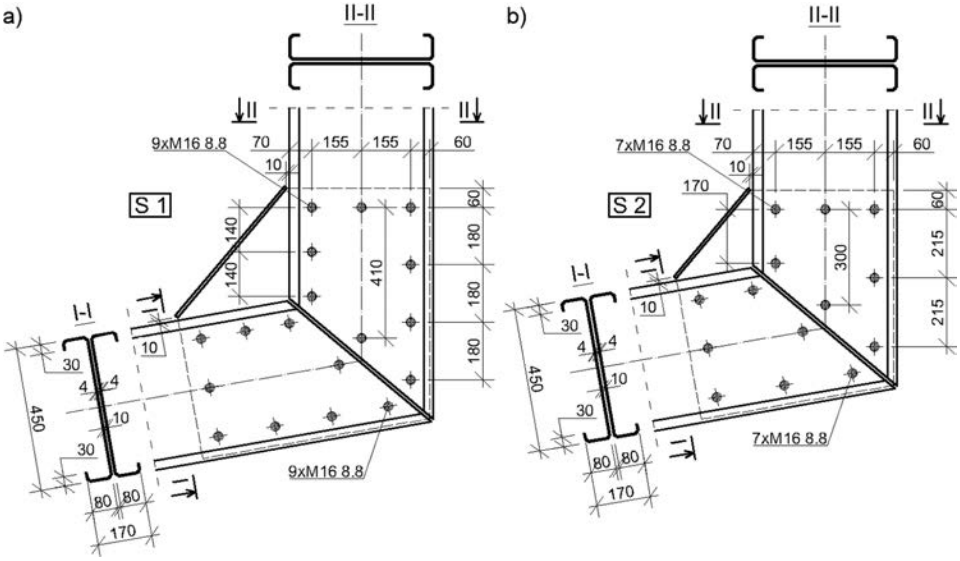

Fig. 2. Joint specimen geometry for types a) S 1 and b) S 2

nearby the joint area and the welded inner flange of the gusset plate. Rotations between the two members and the gusset plate were recorded with two inclinometers. In addition, the in plane displacements of bolts and joint area was measured by the optical system ARAMIS 2D. The instrumentation of the testing stand is presented in Fig. 3.

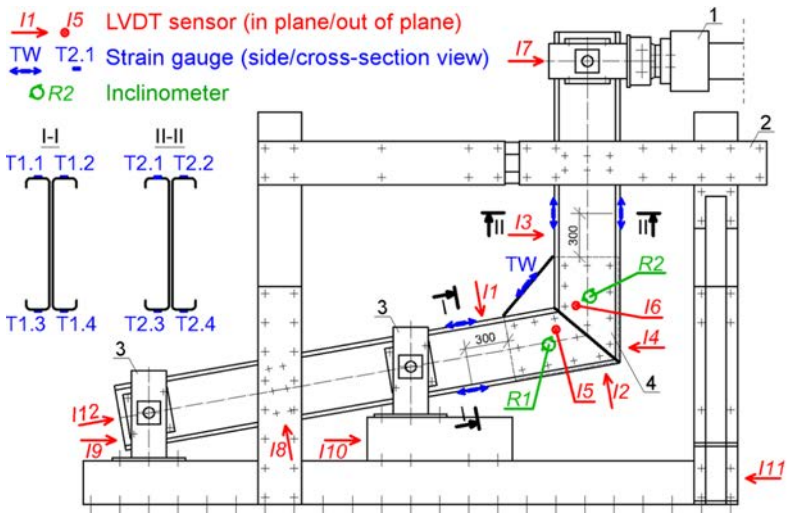

Fig. 3. The instrumentation of the testing stand: 1 – hydraulic jack, 2 – rigid frame, 3 – simple supports, 4 – specimen

2.4. Testing procedure

Each presented joint geometry was tested under 3 loading histories: 2 monotonic and 1 cyclic. Monotonic tests were conducted distinguishing between two opposite directions of loading: positive (+) and negative (–) bending, resulting in "closing" and "opening" of the joint, respectively (Fig. 1a). The loading was applied with the control of the displacement rate of 1 mm/min at loading and 2 mm/min at unloading. Cyclic loading history was based on ECCS publication [21]. The base for the derivation of the loading history was the value of the reference displacement e_y, which was obtained from monotonic tests. The method of determining this parameter is presented in Fig. 4. The cyclic loading pattern starts with 5 cycles with increasing level of loading range. Then the loading is applied in the blocks of three similar cycles with an increasing trend. The loading histories for experimental testing are presented in Fig. 5. The summary of the testing programme is presented in Table 1.

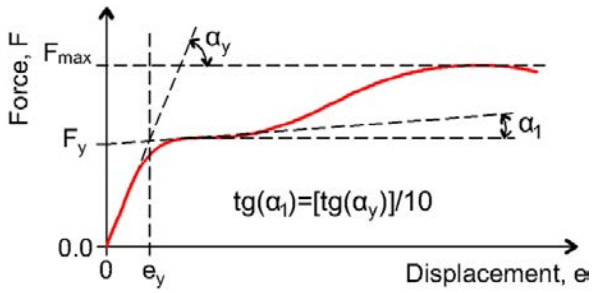

Fig. 4. Method of determining the referential displacement e_y from force-displacement diagram

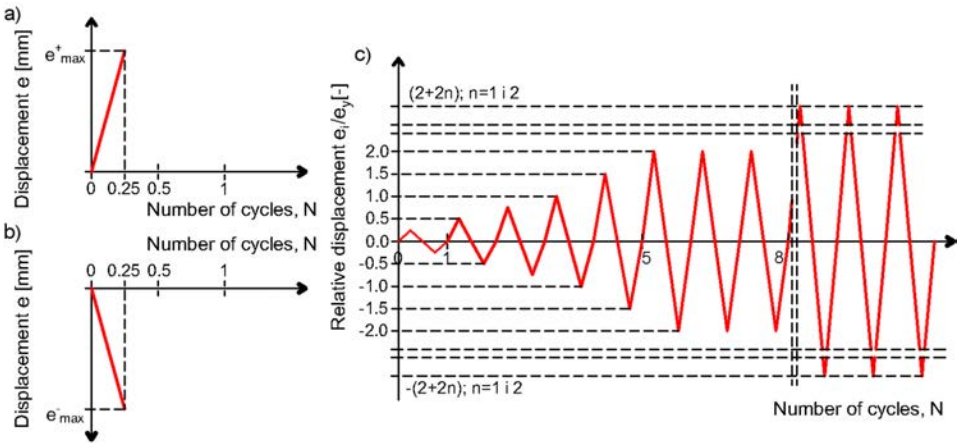

Fig. 5. Loading history patterns for monotonic tests including a) positive (+) and b) negative (–) direction of loading and c) cyclic tests based on ECCS publication [21]

Table 1. Summary of testing programme

Joint geometry	Specimen symbol	Loading history	Loading direction
S 1	S 1.1	Monotonic	Positive (+)
	S 1.2	Monotonic	Negative (–)
	S 1.3	Cyclic (ECCS)	Variable (±)
S 2	S 2.1	Monotonic	Positive (+)
	S 2.2	Monotonic	Negative (–)
	S 2.3	Cyclic (ECCS)	Variable (±)

3. Experimental tests results

3.1. Structural properties of joints from monotonic tests

The mechanical steel properties of the test pieces taken from CFS members and gusset plate are summarised in Table 2.

Table 2. Mechanical properties of steel from test pieces

Origin of the test piece	Test piece thickness [mm]	Number of test pieces	Mean value of yield strength f_y [MPa]	Mean value of ultimate strength f_u [MPa]	Mean value of elongation at ultimate strength ε_u [%]
CFS members	4	5	403.4	527.8	15.8
Gusset plate	10	5	393.7	517.6	16.5

The experimental moment-rotation response of the joints obtained from monotonic tests is presented in Fig. 6. Moment values were determined as the product of the applied force F to the constant lever arm r taken at zero load (1.9 m). The rotation of the joint ϕ was defined as the difference in rotation measured at the centre of gravity of the bolt system on the vertical (ϕ_{R2}) and horizontal (ϕ_{R1}) members respectively.

The moment-rotation response of the joints from monotonic tests shows quite similar trend. The specimens demonstrated significant initial stiffness, followed by a plateau with small increase of moment alongside large rotation. Slight stiffening of the joint was observed at the final stage before reaching maximum moment. Maximum moments were obtained at significant rotation of joints in all analysed cases (0.022÷0.044 radians). These values greatly exceed the total rotation that can occur in steel frame joints in persistent design situation, which is usually limited to 0.01 radians [22].

Maximum experimental moment $M_{\max}$, experimental plastic moment resistance M_{pl} and initial stiffness $S_{j,\mathrm{ini}}$ of the joints were determined on the basis of monotonic tests. The method of evaluation of these properties is presented in Fig. 7. The summary of the experimental results from monotonic tests is presented in Table 3.

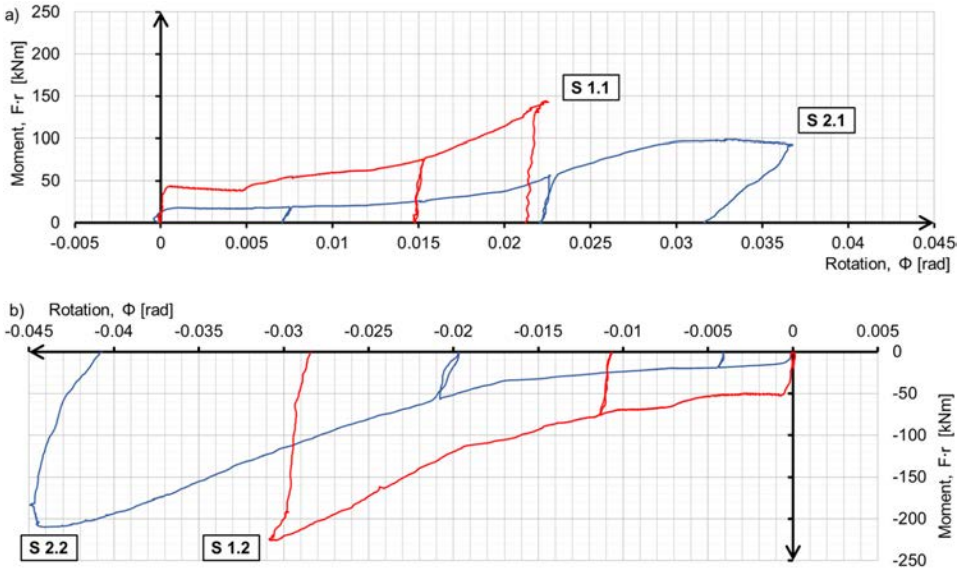

Fig. 6. Experimental moment-rotation response for joints subjected to a) positive (+) and b) negative (–) direction of loading

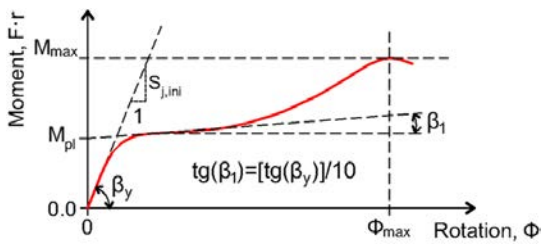

Fig. 7. Method of determining maximum experimental moment $M_{\max}$, experimental plastic moment resistance M_{pl} and initial stiffness $S_{j,\mathrm{ini}}$

Table 3. Summary of experimental results from monotonic tests of joints

Specimen symbol	Loading direction	Maximum experimental moment $M_{\max}$ [kN·m]	Experimental plastic moment resistance M_{pl} [kN·m]	Initial stiffness $S_{j,\mathrm{ini}}$ [kN·m/rad]
S 1.1	Positive (+)	144.2	39.3	158 289
S 1.2	Negative (–)	–226.0	–47.1	76 423
S 2.1	Positive (+)	99.1	15.4	37 321
S 2.2	Negative (–)	–209.9	–12.3	75 850

On the grounds of experimental results, the joints were classified by resistance and stiffness based on EN-1993-1-8 standard [6]. It should be noted, that due to small number of specimens and no repetitions of testing specimens with the same dimensions, the presented classification has only a qualitative value. In order to classify the tested joints, a referential 10 m span portal frame was assumed. Furthermore, the experimental plastic moment resistance of joints M_{pl} was adopted as relevant for the purposes of the classification. The theoretical bending resistance based on the effective section modulus $M_{c,Rk,\mathrm{eff}}$ was taken as the reference resistance due to class 4 of the cross section. A graphical representation of the boundaries of joint classification is shown in Fig. 8. The summary of the classification of joints is presented in Table 4.

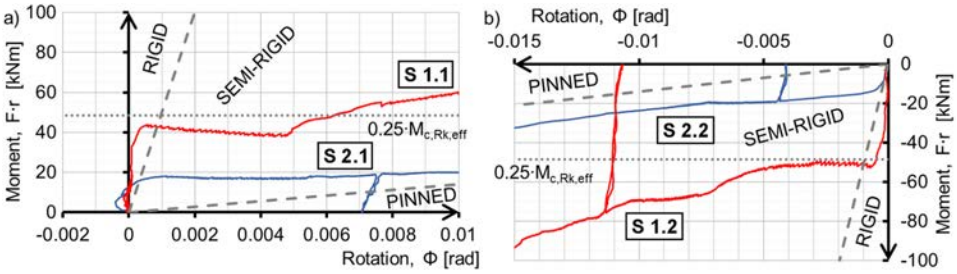

Fig. 8. Boundaries of the classification of joints on the moment-rotation diagram for specimens under a) positive (+) and b) negative (–) direction of bending

Table 4. Summary of the evaluation of joints classification from monotonic tests

Spec. symbol	Boundaries of classification by resistance [kN·m]		Exp. plast. moment resistance of the joint M_{pl} [kN·m]	Joint classification by resistance	Boundaries of classification by stiffness [kN·m/rad]		Initial stiffness $S_{j,\mathrm{ini}}$ [kN·m/rad]	Joint classification by stiffness
	Pinned	Full-Strength			Pinned	Rigid		
S 1.1	48.5	194.0	39.3	Pinned	1404	70193	158 289	Rigid
S 1.2			–47.1	Pinned			76 423	Rigid
S 2.1			15.4	Pinned			37 321	Semi-rigid
S 2.2			–12.3	Pinned			75 850	Rigid

The sources of joint deformation were observed during the test thanks to the usage of ARAMIS optical system. The deformability of the joint resulted from the rotation of the two connections between the gusset plate and each member and the deformability of the gusset plate itself. An evaluation of the contribution of individual components was performed by optical registration of the rotation of each part of the joint. Firstly, the absolute values of rotation were read for gusset plate-to-rafter and gusset plate-to-column connections ($\phi_{H,a}$ and $\phi_{V,a}$) and the gusset plate itself ($\phi_{gp,a}$). The rotation resulting from the deformability of the gusset plate was also extracted from the readings. On that basis, the rotation of

the gusset plate excluding its deformability was determined ($\phi_{gp,a-d}$). The course and graphical representation of all these rotations for S 2.2 specimen are shown in Fig. 9a and 9b, respectively. On these grounds, a proportional share of the rotation of each joint component was imposed on the moment-rotation diagram (see Fig. 10a). The majority of total rotation of joint was induced by the deformation of the two bolted connections. The values were quite equal during the test and varied between 40 and 46% for each connection. The deformability of the gusset plate itself, which was loaded in tension or compression, appeared to be responsible for a minor part of the rotation of the joint. This component's contribution to the total rotation was decreasing as the loading progressed. As a conclusion, a mechanical model of the studied joint can be presented as three rotational springs connected in series with stiffnesses $S_{j,V}$, $S_{j,H}$ and $S_{j,gp}$. (see Fig. 10b).

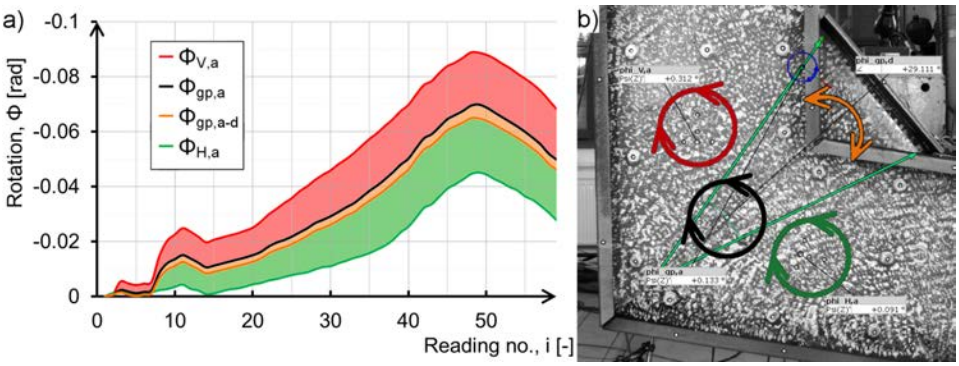

Fig. 9. a) The course of rotation of joint components during the test and b) graphical representation of each rotation for S 2.2 specimen from ARAMIS software (description in the text)

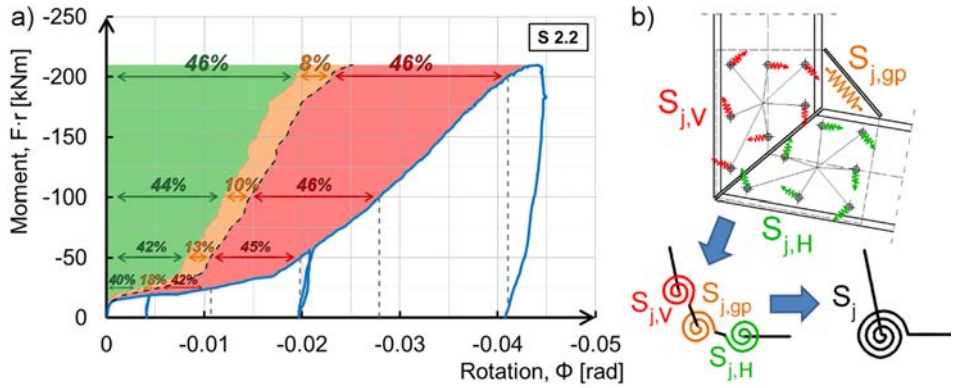

Fig. 10. a) Share of rotations of each component on moment-rotation diagram for S 2.2 specimen and b) mechanical representation of the tested joints (description in the text)

The observed failure of joints varied for different direction of loading. Specimens subjected to positive (+) direction of moment failed due to lateral buckling in the joint

area (Fig. 11a,b). Considering specimens subjected to negative (–) direction of bending, the failure was manifested as large deformations developed in the compressed parts of the horizontal member, nearby the gusset plate (Fig. 11c). Moreover, ovalization of holes was observed after the disassembly of the specimens. It occurred in the holes located at a larger distance from the centre of the gravity of bolts arrangement. The ovalization was mostly noticeable in the webs of the members rather than the gusset plate (Fig. 11d,e).

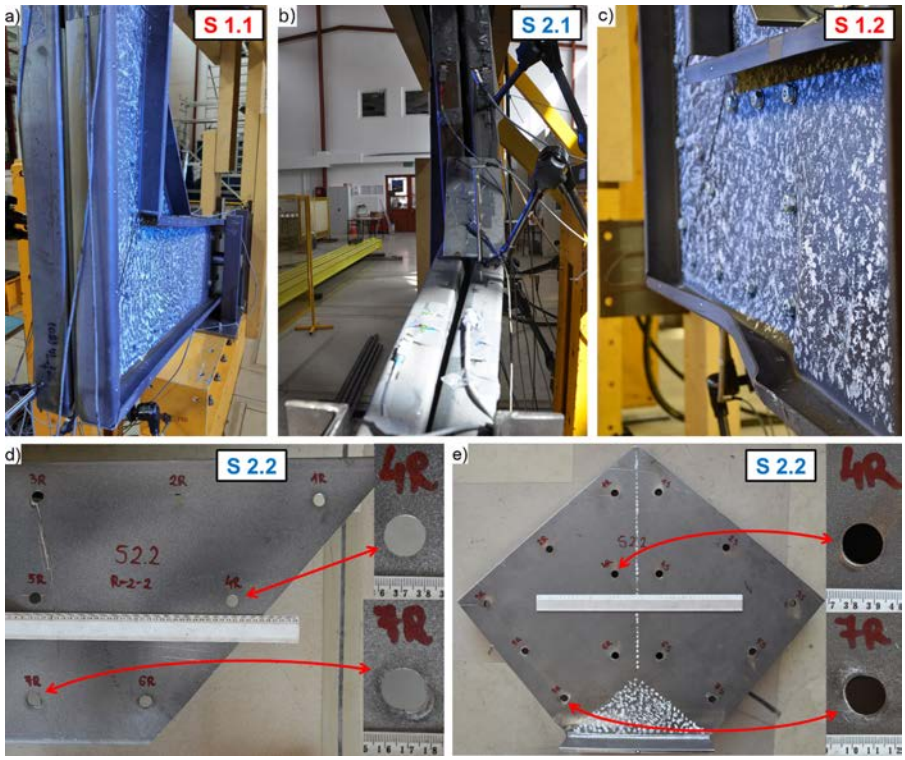

Fig. 11. Failure modes of the tested joints (description in the text)

3.2. Deterioration of structural properties of joints under cyclic tests

The loading ranges for cyclic tests were based on a multiple of the introduced reference displacement value e_y. Thus, the level of loading at each range is described by the relative displacement range μ_i:

$$\mu_i = e_i / e_y \tag{3.1}$$

where: e_i – value of displacement at given block of loading, e_y – reference value of displacement corresponding to F_y force from monotonic tests.

The moment rotation response for joints under cyclic loading is presented in Fig. 12.

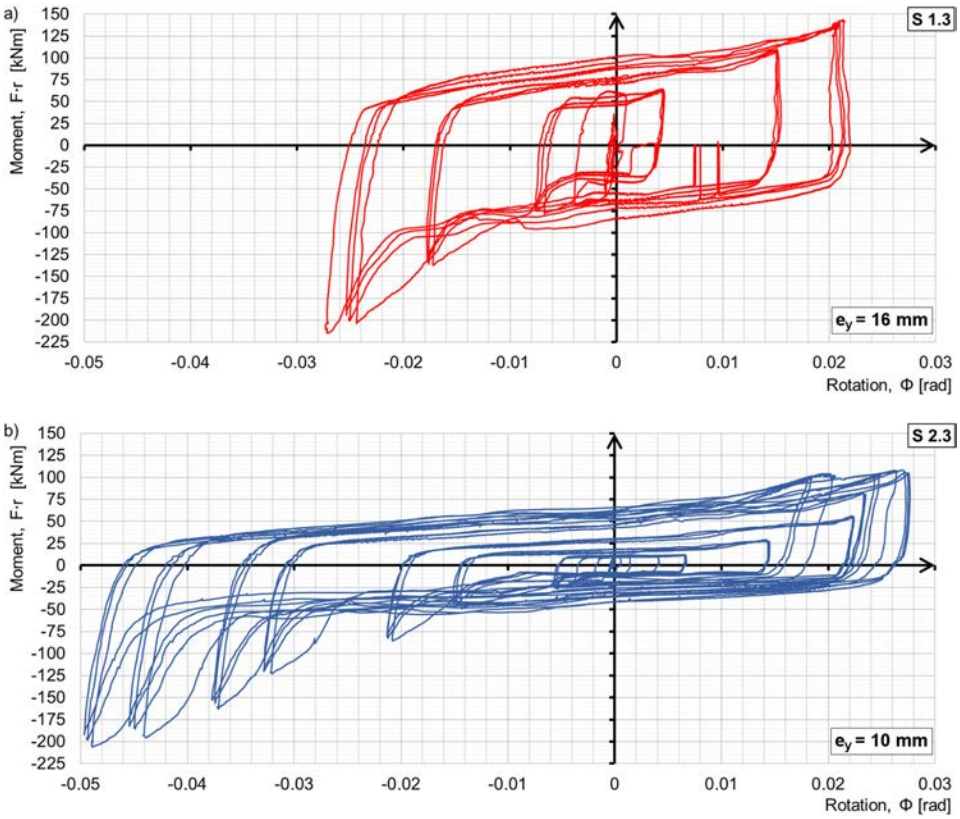

Fig. 12. Experimental moment-rotation response from cyclic tests for a) S 1.3 and b) S 2.3 specimen

The load cycles were applied until a load drop was reached and clear failure of the specimen was observed. Displacements equivalent to $6e_y$ and $14e_y$ were achieved for sample S 1.3 and S 2.3 respectively. In order to interpret the results of cyclic tests, several reference values from monotonic tests were utilized. Experimental plastic moment resistances M_{pl} were adopted as a basis for the evaluation of deterioration of resistance. As with the monotonic tests, in view of the limited number of specimens, the assessment of drop of structural properties from cyclic tests shall be considered in terms of qualitative value.

The deterioration of bending resistance of the connection under variable loading might be described as a decrease (or increase) of the moment value alongside subsequent cycles. Firstly, the quantity of this phenomenon was evaluated in the relation to above reference moment value M_{pl} and introduced as the resistance ratio $\varepsilon(\mu)$:

$$\varepsilon(\mu_i) = M_{i,\min}/M_{\mathrm{pl}} \tag{3.2}$$

where: $M_{i,\min}$ – minimum moment value in the group of 3 cycles in one block of loading.

Parameter describing the deterioration of resistance alongside one block of loading was introduced as the resistance drop ratio $\varepsilon^*(\mu)$:

$$\varepsilon^*(\mu_i) = M_{i,3}/M_{i,1} \tag{3.3}$$

where: $M_{i,3}$, $M_{i,1}$ – maximum moment values in third and first cycle in one block of loading, respectively.

The analyzed connections were also suspected of a decrease of stiffness under variable type of loading. As described earlier, this phenomenon has an essential meaning for serviceablility of the structure. The stiffness values obtained from cyclic tests were compared to the initial stiffness $S_{j,\text{ini}}$ from monotonic tests. The deterioration of stiffness was evaluated on the grounds of the stiffness ratio $\xi(\mu)$:

$$\xi(\mu_i) = S_{j,i,\min}/S_{j,\text{ini}} \tag{3.4}$$

where: $S_{j,i,\min}$ – minimum initial stiffness value in the group of 3 cycles in one block of loading.

Similarly, the stiffness drop alongside one block of loading was introduced as the resistance drop ratio $\xi^*(\mu)$:

$$\xi^*(\mu_i) = S_{j,i,3}/S_{j,i,1} \tag{3.5}$$

where: $S_{j,i,3}$, $S_{j,i,1}$ – initial stiffness values in third and first cycle in one block of loading, respectively.

The way of determining the values of moment and stiffness for the evaluation of introduced ratios from cyclic tests is shown in Fig. 13. The trend of quantities describing the deterioration of resistance and stiffness versus the relative displacement range are presented in Fig. 14 and 15, respectively.

The values of resistance ratio $\varepsilon(\mu)$ showed quite linear course. In this case the parameter is unreliable when it comes to the evalutaion of deteroration of resistance. It results from the fact that the derived reference values of moment M_y were multiple times lower than the maximum moment that might be obtained alongside larger rotations. However the

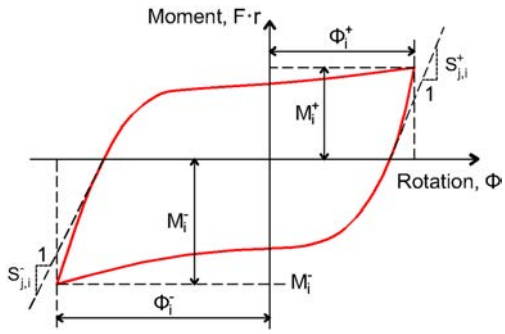

Fig. 13. Method of determining basic moment and stiffness values for the evaluation of deterioration of structural properties from cyclic tests

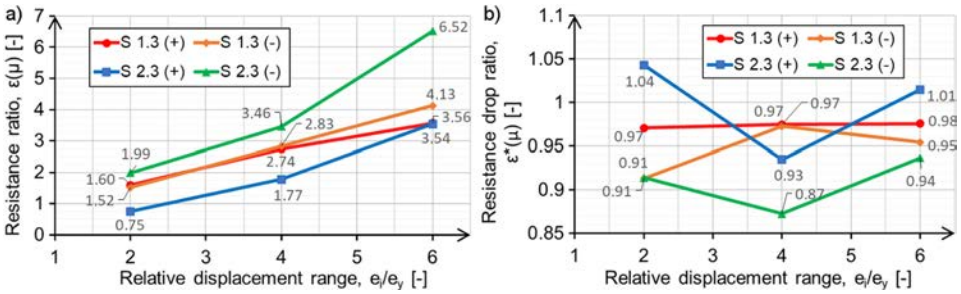

Fig. 14. The trend of a) resistance ratio $\varepsilon(\mu)$ and b) resistance drop ratio $\varepsilon*(\mu)$ versus relative displace-ment range from cyclic tests distinguishing positive (+) and negative (–) direction of loading

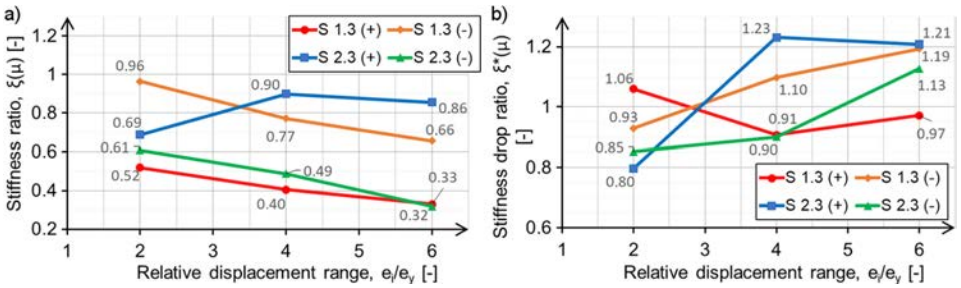

Fig. 15. The trend of a) stiffness ratio $\xi(\mu)$ and b) stiffness drop ratio $\xi*(\mu)$ versus relative displace-ment range from cyclic tests distinguishing positive (+) and negative (–) direction of loading

resistance drop ratio $\varepsilon*(\mu)$ exposed some invariance of resistance alongside each block of loading. The trend shows that the deterioration of resistance is noted in the majority of specimens. Nonetheless the quantity of deterioration does not increase alongside the relative displacement range. It should be noted, that larger drop of resistance was observed in negative (–) loading direcion, which did not cause the lateral buckling of the joint areas.

Regarding the flexibility of the joints, the introduced stiffness ratio $\xi(\mu)$ revealed a decreasing trend of the stiffness in successive blocks of loading. None of the specimens reached the reference values of initial stiffness $S_{j,\mathrm{ini}}$ from monotonic tests. The decrease of this parameter varied between 4% and 68%, which shall be evaluated as very significant drop. On the other hand, stiffness drop ratio did not reveal any decrease of flexibility alongside each block of loading. What is more, some of the specimens gained stiffness at certain loading range within a single blocks.

4. Summary and conclusions

The investigation of bolted lap joints of eaves connection in CFS portal frame under different types of loading is presented in this paper. Two joint geometries were tested in cases of bending under monotonic and cyclic loading. Basic structural properties were obtained from

monotonic tests and taken as reference values for the evaluation of the results from cyclic tests. Several quantities of the deterioration of bending moment resistance and joint stiffness were determined. Considering the limited number of specimens for each type of loading, due to financial constraints, the evaluation of the experimental results has only a qualitative value. However, it shows the general behaviour of such type of joints subjected to bending.

Monotonic tests showed quite similar moment–rotation $M-\phi$ relationships for all joints under the positive and negative direction of moments. Three stages might be highlighted in the response of tested joints: significant initial stiffness, a plateau characterised by a small increase in moment alongside a large rotation, and slight stiffening of the samples before reaching maximum moment. All joints exhibited a large rotational deformation capacity in the inelastic range. Digital image correlation measurements revealed three following sources of the deformation: rotations of two connections between the gusset plate and each member and the deformability of the gusset plate itself. The great part of the rotation was induced by the bolted connections. Considering an exemplary specimen under negative moment direction, both connections showed a fairly comparable contribution as the test progressed, each achieving a 42÷46% proportion of the joint rotation. The deformability of the gusset plate was responsible for a small part of the total rotation (8÷18%) and its influence was decreasing with increasing load. The rotation values at maximum loading varied between 0.022 and 0.044 radians.

Experimental plastic moment resistances were several times lower than the maximum moments obtained during the tests. Classification by strength, according to criteria given in EN 1993-1-8, shows that tested joints can be classified as pinned. This is due to the fact that channel member profiles are bolted only through the web to the gusset plate – the bending resistance of such solution almost never reaching the full strength of the connected members. The second reason that influences the low bending resistance may be the clearance between the bolt and the bolt hole. The first plateau in $M-\phi$ relationship (the second stage of $M-\phi$ behaviour) determining the experimental plastic bending resistance comes in part from the member slipping between the web and the gusset plate, which begins after reaching the friction limit of individual bolt. Because the bolts were only slightly tightened, their slip resistance was rather low.

Cyclic tests conducted on the basis of ECCS recommendations [21] provided measures of the deterioration of resistance and stiffness of the joints. Several quantities were introduced in order to assess these phenomena with reference to monotonic test results and in terms of the variation over subsequent cycles of each loading block. The moment resistance drop was observed in successive cycles in the same displacement range. However, the quantity of the deterioration did not increase with the loading range. The initial stiffness from monotonic tests was not reached over any range of loading in any of the samples. Furthermore, the stiffness values were decreasing significantly in each subsequent load range. In at least half of the cases, the drop exceeded 30% and reached over 60% in most extreme scenario. This trend can be considered as a significant deterioration of joint stiffness in reference to the initial stiffness at first loading. Taking into account the variation of stiffness alongside the same loading range, the drop was observed only in a few cases. Furthermore, the majority of joints gained stiffness through the following cycles repeated in a single load block.

References

[1] J. Bródka, A. Kozłowski, I. Ligocki, J. Łaguna, and L. Ślęczka, *Design and calculating of connections and joints of steel structures*, vol. 2. Rzeszów, Poland: Polish Technical Publisher, 2013 (in Polish).

[2] A.M. Wrzesien and J.B.P. Lim, "Cold-formed steel portal frame joints a review", in *Proceedings of the 19th International Specialty Conference on Cold-Formed Steel Structures*. St. Louis, Missouri, USA, 2008, pp. 591–606.

[3] P. Krystosik, "On the columns buckling length of unbraced steel frames with semi-rigid joints", *Archives of Civil Engineering*, vol. 67, no. 1, pp. 539–556, 2021, doi: 10.24425/ace.2021.136488.

[4] A. Kozłowski, "Guidelines for predesign of steel frames with semi-rigid joints", in *EUROSTEEL 2005. Proceedings of the 4th European Conference on Steel and Composite Structures: Research-Eurocodes-Practice*. Maastricht, The Netherlands, 2005, vol. C. pp. 4.10-197–4.10-205.

[5] Ž. Bučmys and A. Daniūnas, "Rectangular gusset plate behaviour in cold-formed I-type steel connections", *Archives of Civil Engineering*, vol. 63, no. 2, pp. 3–21, 2017, doi: 10.1515/ace-2017-0013.

[6] EN 1993-1-8 Eurocode 3 – Design of steel structures – Part 1–8: Design of joints. CEN, Brussels, 2006.

[7] R. Klich, A. Wojnar, and A. Kozłowski, "Experimental tests of corner joints used in steel thin-walled frames", in *Progress in steel and composite structures: proceedings of the 12th International Conference on Metal Structures*. Wrocław, Poland, 2011.

[8] D. Dubina, A. Stratan, and Z. Nagy, "Full – scale tests on cold-formed steel pitched-roof portal frames with bolted joints", *Advanced Steel Construction*, vol. 5, no. 2, pp. 175–194, 2009, doi: 10.18057/IJASC.2009.5.2.7.

[9] M. Firdaus, A. Saggaff, M. Tahir, S.P. Ngian, K. Aminuddin, and F. Usman, "Experimental study of slip-in haunched gusset plate connection for double lipped cold- formed steel section", *International Journal of Scientific & Technology Research*, vol. 8, no. 12, pp. 3215–3221, 2019.

[10] E. Bernatowska and L. Ślęczka, "Net section resistance of steel angles connected by one leg", *Archives of Civil Engineering*, vol. 68, no. 4, pp. 275–291, 2022, doi: 10.24425/ace.2022.143038.

[11] J.B.P. Lim and D.A. Nethercot, "Ultimate strength of bolted moment-connections between cold-formed steel members", *Thin-Walled Structures*, vol. 41, no. 11, pp. 1019–1039, 2003, doi: 10.1016/S0263-8231(03)00045-4.

[12] F. Öztürk and S. Pul, "Experimental and numerical study on a full scale apex connection of cold-formed steel portal frames", *Thin-Walled Structures*, vol. 94, pp. 79–88, 2015, doi: 10.1016/j.tws.2015.04.004.

[13] X. Chen, H.B. Blum, K. Roy, P. Pouladi, A. Uzzaman, and J.B.P. Lim, "Cold-formed steel portal frame moment-resisting joints: Behaviour, capacity and design", *Journal of Constructional Steel Research*, vol. 183, 2021, doi: 10.1016/j.jcsr.2021.106718.

[14] L.H. Martin and S. Robinson, "Experiments to investigate parameters associated with the failure of triangular steel gusset plates", in *Joint in structural steelwork*, J. H. Howlett, W. M. Jenkins, and R. Stainsby, Eds. Pentech Press, 1981.

[15] EN 1090-2 Execution of steel structures and aluminium structures – Part 2: Technical requirements for steel structures. CEN, Brussels, 2018.

[16] J. Henriques, J.-P. Jaspart, and L. Silva, "Ductility requirements for the design of bolted lap shear connections in bearing", *Advanced Steel Construction*, vol. 10, no. 1, pp. 33–52, 2014, doi: 10.18057/ijasc.2014.10.1.3.

[17] J. Ye, S. Mojtabaei, and I. Hajirasouliha, "Seismic performance of cold-formed steel bolted moment connections with bolting friction-slip mechanism", *Journal of Constructional Steel Research*, vol. 156, pp. 122–136, 2019, doi: 10.1016/j.jcsr.2019.01.013.

[18] A.B. Sabbagh, M. Petkovski, K. Pilakoutas, and R. Mirghaderi, "Cyclic behaviour of bolted cold-formed steel moment connections: FE modelling including slip", *Journal of Constructional Steel Research*, vol. 80, pp. 100–108, 2013, doi: 10.1016/j.jcsr.2012.09.010.

[19] Y.N. Saleh, H. H. Elanwar, M.T. Hanna, and S.A. Mourad, "Assessment of frame corner connections subjected to cyclic loading in cold formed steel sections", *Journal of Constructional Steel Research*, vol. 199, 2022, doi: 10.1016/j.jcsr.2022.107601.

[20] J. Ye, G. Quan, X. Yun, X. Guo, and J. Chen, "An improved and robust finite element model for simulation of thin-walled steel bolted connections", *Engineering Structures*, vol. 250, 2022, doi: 10.1016/j.engstruct.2021.113368.

[21] ECCS, *Recommended testing procedure for assessing the behaviour of structural steel elements under cyclic loads*. European Convention for Constructional Steelwork, no. 45, 1986.

[22] L. Ślęczka, *Shaping and analysis of selected steel frame joints subjected to variable actions*. Rzeszów, Poland: Publishing House of the Rzeszow University of Technology, 2013 (in Polish).

Badania doświadczalne stalowych, zakładkowych węzłów śrubowych w stalowych konstrukcjach giętych na zimno pod obciążeniem monotonicznym i cyklicznym

Słowa kluczowe: kształtowniki gięte na zimno, obciążenie cykliczne, połączenia śrubowe zakładkowe, sztywność początkowa, węzły stalowe

Streszczenie:

Węzły w stalowych konstrukcjach szkieletowych z elementów giętych na zimno są zwykle projektowane jako śrubowe zakładkowe z blachą węzłową. W odróżnieniu od wariantu doczołowego, powszechnego w konstrukcjach z kształtowników walcowanych na gorąco, obciążenie jest w nich przekazywane poprzez ścinanie śrub i docisk do ścianek elementów. Ich projektowanie może nastręczać trudności jeśli chodzi o przewidywanie właściwości strukturalnych związanych z obrotem, a więc sztywności i ciągliwości. Wynika to z niekorzystnych i trudnych w analizie przemieszczeń wewnątrz złączy śrubowych. Składają się na nie luzy występujące pomiędzy trzpieniem śruby a otworem oraz owalizacja otworów pod obciążeniem spowodowana małą nośnością cienkich ścianek na docisk. Wiele dotychczas przeprowadzonych badań doświadczalnych wykazało, że wspomniane wpływy prowadzą do innego zachowania się tego typu węzłów w porównaniu z wariantem doczołowym. Zagadnienia te mogą okazać się szczególnie niekorzystne przy działaniu obciążeń zmiennych, prowadzących do potencjalnej degradacji właściwości strukturalnych. W niniejszym artykule przedstawiono podsumowanie autorskich badań doświadczalnych śrubowych węzłów zakładkowych, pełniących funkcję połączenia okapowego w stalowej ramie portalowej z kształtowników giętych na zimno. Celem badań było określenie ich zachowania się pod wpływem obciążeń monotonicznych i cyklicznych ze zwróceniem szczególnej uwagi na potencjalną degradację nośności i sztywności. Nowością opisaną w artykule jest zastosowanie techniki DIC (Digital Image Correlation), która pozwoliła na jakościową i ilościową identyfikację źródełodkształcalności węzłów.

Badania przeprowadzono na stanowisku doświadczalnym przygotowanym dla węzłów narożnych konstrukcji stalowych. Elementy próbne składały się z fragmentu rygla i słupa ramy portalowej (odpowiednio element pionowy i poziomy), połączonych w sposób zakładkowy z wykorzystaniem blachy węzłowej. Siła generująca moment zginający w węźle przykładana było poziomo w swobodnym końcu rygla (element pionowy) dzięki wykorzystaniu siłownika hydraulicznego. Następnie obciążenie przekazywane było na słupek (element poziomy), który byłpołączony pośrednio z podłogą siłową za pomocą dwóch podpór przegubowych.

Badany węzełstanowiłpołączenie elementów o przekroju złożonym z dwóch giętych na zimno ceowników zwróconych stopkami na zewnątrz, odsuniętych od siebie o 10 mm. Wykorzystano kształtowniki o wysokości 450 mm, szerokości pasów 80 mm i szerokości usztywnień brzegowych 30 mm, profilowane z blachy grubości 4 mm. W szczelinie pomiędzy ceownikami zaprojektowano blachę

węzłową o grubości 10 mm, która stanowiła łącznik pomiędzy ryglem a słupkiem. Element ten dodatkowo usztywniono spawanym pasem od wewnętrznej strony naroża. Wszystkie blachy stalowe wykorzystane w elementach próbnych wykonano ze stali gatunku S355. Węzełzrealizowano za pomocą śrub M16 klasy 8.8, które łączyły blachę węzłową i środniki ceowników w obu elementach dochodzących. Do badań przygotowano dwie geometrie próbek różniące się liczbą i rozstawem śrub, a co za tym idzie wielkością blachy węzłowej. W pierwszym i drugim wariancie (S 1 i S 2) zastosowano odpowiednio 18 i 14 łączników. Śruby dokręcono kluczem dynamometrycznym z niewielkim momentem obrotowym równym 60 Nm.

Badania doświadczalne każdego z typów węzłów przeprowadzono pod 3 różnymi historiami obciążenia: dwoma monotonicznymi (z rozróżnieniem zwrotu obciążenia dociążającego i unoszącego, powodującego odpowiednio „zamykanie" i „otwieranie" węzła) oraz cykliczną. Protokół dla ostatniej z nich określono na podstawie publikacji ECCS nr 45 (ECCS, 1986). Początkowo zakres zmienności był zwiększany po każdym cyklu, zaś po osiągnięciu określonej wartości amplitudy cykle powtarzano trzykrotnie na każdym kolejnym poziomie obciążenia. Wszystkie próby doświadczalne prowadzone były przy sterowaniu przemieszczeniem tłoka siłownika. Przez wzgląd na ograniczoną liczbę próbek i brak powtórzeń dla poszczególnych typów węzłów pod danym rodzajem obciążenia, przedstawiona ocena uzyskanych wyników ma charakter wyłącznie jakościowy.

Badania monotoniczne wykazały dość podobny przebieg zależności moment-obrót węzłów pomimo różnych właściwości strukturalnych dla każdego ze zwrotów momentu zginającego. Elementy próbne odznaczały się znaczną sztywność początkową, po której następował etap charakteryzujący się niemal stałą wartością momentu utrzymującą się przy postępującym obrocie. Przed osiągnięciem maksymalnego momentu nachylenie krzywej moment-obrót wzrastało z powodu nieznacznego usztywnienia węzła. Wszystkie próbki wykazywały dużą zdolnością do obrotu w zakresie pozasprężystym. Pomiary optyczne wykonane aparaturą do cyfrowej korelacji obrazu ujawniły trzy główne źródła deformacji węzła. Za znaczną część obrotu odpowiadały połączenia śrubowe występujące pomiędzy odpowiednio elementami rygla i słupka a blachą węzłową. Dla przykładowej próbki wariantu S 2 pod obciążeniem „unoszącym" odnotowano zbliżony udziałtych składników w całkowitym obrocie węzła na poziomie około 45% dla każdego z nich. Pozostała część wynikała z odkształcalności blachy węzłowej, a jej wpływ malałprzy wzroście obciążenia. Po osiągnięciu maksymalnych momentów zginających zaobserwowano znaczne deformacje w ściskanych częściach elementu poziomego w pobliżu blachy węzłowej. Węzły poddane działaniu obciążenia dociążającego („zamykanie" węzła) osiągnęły mniejsze wartości maksymalnych momentów zginających w stosunku do próbek pod obciążeniem symulującym unoszenie („otwieranie" węzła) ze względu na wyboczenie poprzeczne w obszarze połączeń.

Na podstawie uzyskanych wyników wyznaczono sztywności początkowe oraz plastyczne nośności na zginanie węzłów, które posłużyły do ich sklasyfikowania według normy EN-1993-1-8. Do wyznaczenia przedziałów poszczególnych grup przyjęto teoretyczną nośność efektywnego przekroju poprzecznego i rozpiętość ramy równą 10 m. Za wartości reprezentatywne uznano doświadczalne wartości sztywności początkowej i plastycznej nośności węzła. Pod względem sztywności tylko próbka z większą liczbą śrub pod obciążeniem „zamykającym" spełniła warunek węzła sztywnego, podczas gdy pozostałe zostały sklasyfikowane jako półsztywne. Niemniej jednak, biorąc pod uwagę podatną odpowiedź połączeń po etapie początkowym, takie przyporządkowanie może być wątpliwe. W przypadku nośności wszystkie próbki przyporządkowano do grupy przegubowych, gdyż żadna z nich nie wykazała się nośnością większą niż 25% teoretycznej nośności na zginanie łączonego przekroju poprzecznego. Należy zaznaczyć, że doświadczalne nośności plastyczne były wielokrotnie mniejsze od maksymalnych wartości momentów uzyskanych w badaniu. Podobna proporcja tyczyła się również kątów obrotu, przy których osiągane były obie wielkości.

Na podstawie badań cyklicznych dokonano oceny degradacji właściwości strukturalnych. W tym celu wprowadzono kilka wielkości, które stanowiły odniesienie do wyników badań monotonicznych lub opisywały zmiany w cyklach powtarzanych na tym samym poziomie obciążenia. Wielkość i przebieg degradacji różniłsię w zależności od rozpatrywanej właściwości. Spadek nośności węzłów obserwowano przy kolejnych powtórzeniach w tym samym zakresie zmienności. Wielkość degradacji nie wzrastała jednak wraz ze zwiększaniem się amplitudy obciążenia. Sztywność początkowa z badań monotonicznych nie została osiągnięta przy żadnym z zakresów zmienności w żadnej z próbek. Co więcej, w każdym kolejnym bloku powtórzeń na kolejnych poziomach obciążenia wartości sztywności znacząco malały. W co najmniej połowie przypadków spadek ten przekroczył 30%, a w skrajnym scenariuszu osiągnął ponad 60%. Przedstawiony trend można uznać za znaczną degradację sztywności połączenia w odniesieniu do sztywności początkowej z prób monotonicznych. Biorąc pod uwagę zmienność tego parametru dla kolejnych powtórzeń przy niezmiennej amplitudzie, nieznaczny spadek zaobserwowano tylko w kilku przypadkach. Większość węzłów wykazała się wręcz zwiększeniem sztywności w ostatnim cyklu danego bloku powtórzeń.

Received: 2023-06-02, Revised: 2023-07-20